Structure and Photophysics of *β*-Octafluoro-*meso*-tetraarylporphyrins§

Valeriy V. Smirnov,† Eric K. Woller,† Dereck Tatman,‡ and Stephen G. DiMagno*,†

Department of Chemistry, University of Nebraska-Lincoln, Lincoln, Nebraska 68588-0304, and
Department of Chemistry and Biochemistry, Arizona State University, Tempe, Arizona 85287-1604

The structure of THF-coordinated [2,3,7,8,12,13,17,18-octafluoro-5,10,15,20-tetraphenylporphinato]zinc, Zn(F$_8$-TPP)·THF, and photophysical studies of 2,3,7,8,12,13,17,18-octafluoro-5,10,15,20-tetraphenylporphyrin, F$_8$TPP, Zn(F$_8$TPP), 2,3,7,8,12,13,17,18-octafluoro-5,10,15,20-tetrakis(pentafluorophenyl)porphyrin, F$_{28}$TPP, and [2,3,7,8,-12,13,17,18-octafluoro-5,10,15,20-tetrakis(pentafluorophenyl)porphinato]zinc, Zn(F$_{28}$TPP), in benzonitrile, are reported. A key point from these studies is that the octafluorinated F$_8$TPP and perfluorinated F$_{28}$TPP porphyrins possess similar absorption spectra, but dissimilar X-ray crystal structures and disparate photophysical characteristics. These data cannot be easily accommodated within currently accepted theories which relate macrocycle distortion and optoelectronic properties.

Introduction

Recent X-ray crystal structure determinations of light harvesting antenna and reaction center proteins show porphyrinic pigments constrained to adopt nonplanar geometries by polypeptide matrices.[1−4] It is an unresolved issue whether the observed pigment conformational diversity is integral to the function of these proteins or if it is simply a product of evolutionary happenstance. In principle, nonplanar distortion of porphyrin rings could serve as a means by which nature modulates the redox and photophysical properties of these important pigments.[5,6]

To understand the functional importance, if any, of the observed landscape of pigment conformational diversity in natural systems, comparative electrochemical, spectroscopic, and photophysical studies of structurally characterized planar and nonplanar porphyrins are required. Many conformationally constrained model compounds have been synthesized in an effort to delineate the electronic consequences of porphyrin ring

distortion, and comprehensive reviews have been published recently.[7−9] Several of these nonplanar porphyrins have been subjected to detailed photophysical studies.[10−17] Studies of electron-rich, sterically encumbered nonplanar porphyrins[18−22] demonstrate that these compounds exhibit bathochromically shifted absorption spectra, reduced S$_1$ lifetimes (τ_f), small quantum yields of fluorescence (ϕ_f), broad emission bands with large Stokes shifts, and increased internal conversion rate constants (k_{ic}) relative to standard planar porphyrins, such as 5,10,15,20-tetraphenylporphyrin (TPP) and 2,3,7,8,12,13,17,-

* To whom correspondence should be addressed.
† University of Nebraska.
‡ Arizona State University.
§ Abbreviations used in this manuscript are as follows: DPP, 2,3,5,7,8,-10,12,13,15,17,18,20-dodecaphenylporphyrin; TPP, 5,10,15,20-tetraphenylporphyrin; OEP, 2,3,7,8,12,13,17,18-octaethylporphyrin; T(*t*-Bu)P, 5,-10,15,20-tetrakis(*tert*-butyl)porphyrin; OETPP, 5,10,15,20-tetraphenyl-2,3,-7,8,12,13,17,18-octaethylporphyrin; TR$_f$P, 5,10,15,20-tetrakis(perfluoro-alkyl)porphyrin; TC$_3$F$_7$P, 5,10,15,20-tetrakis(heptafluoropropyl)porphyrin; F$_8$TPP, 5,10,15,20-tetraphenyl-2,3,7,8,12,13,17,18-octafluoroporphyrin; F$_{28}$-TPP, 5,10,15,20-tetrakis(pentafluorophenyl)-2,3,7,8,12,13,17,18-octafluo-roporphyrin; TFPP, 5,10,15,20-tetrakis(pentafluorophenyl)porphyrin; Cl$_8$-TFPP, 5,10,15,20-tetrakis(pentafluorophenyl)-2,3,7,8,12,13,17,18-octachlor-oporphyrin; Br$_8$TFPP, 5,10,15,20-tetrakis(pentafluorophenyl)-2,3,7,8,12,-13,17,18-octabromoporphyrin.

(1) Deisenhofer, J.; Michel, H. *Science* **1989**, *245*, 1463−1473.
(2) Deisenhofer, J.; Michel, H. *Angew. Chem., Int. Ed. Engl.* **1989**, *28*, 829−847.
(3) Freer, A.; Prince, S.; Sauer, K.; Papiz, M.; Hawthornthwaite-Lawless, A.; McDermott, G.; Cogdell, R.; Isaacs, N. W. *Structure* **1996**, *4*, 449−462.
(4) Tronrud, D. E.; Schmid, M. F.; Matthews, B. W. *J. Mol. Biol.* **1986**, *188*, 443−454.
(5) Barkigia, K. M.; Chantranupong, L.; Smith, K. M.; Fajer, J. *J. Am. Chem. Soc.* **1988**, *110*, 7566−7567.
(6) Shelnutt, J. A.; X.-Z., S.; Ma, J.-G.; Jia, S.-L.; Jentzen, W.; Medforth, C. J. *Chem. Soc. Rev.* **1998**, *27*, 31−41.

(7) Ravikanth, M.; Chandrashekar, T. K. *Struct. Bonding* **1995**, *82*, 105−188.
(8) Senge, M. O. In *The Porphyrin Handbook*; Kadish, K. M., Smith, K. M., Guilard, R., Eds.; Academic Press: New York, 2000; Vol. 1; pp 239−347.
(9) Shelnutt, J. A. In *The Porphyrin Handbook*; Kadish, K. M., Smith, K. M., Guilard, R., Eds.; Academic Press: New York, 2000; Vol. 7; pp 167−223.
(10) Ravikanth, M.; Chandrashekar, T. K. *J. Photochem. Photobiol. A., Chem.* **1993**, *74*, 181−187.
(11) Maiti, N. C.; Ravikanth, M. *J. Chem. Soc., Faraday Trans.* **1996**, *92*, 1095−1100.
(12) Gentemann, S.; Medforth, C. J.; Forsyth, T. P.; Nurco, D. J.; Smith, K. M.; Fajer, J.; Holten, D. *J. Am. Chem. Soc.* **1994**, *116*, 7363−7368.
(13) Gentemann, S.; Medforth, C. J.; Ema, T.; Nelson, N. Y.; Smith, K. M.; Fajer, J.; Holten, D. *Chem. Phys. Lett.* **1995**, *245*, 441−447.
(14) Gentemann, S.; Nelson, N. Y.; Jaquinod, L.; Nurco, D. J.; Leung, S. H.; Medforth, C. J.; Smith, K. M.; Fajer, J.; Holten, D. *J. Phys. Chem. B* **1997**, *101*, 1247−1254.
(15) Goll, J. G.; Moore, K. T.; Ghosh, A.; Therien, M. J. *J. Am. Chem. Soc.* **1996**, *118*, 8344−8354.
(16) Charlesworth, P.; Truscott, T. G.; Kessel, D.; Medforth, C. J.; Smith, K. M. *J. Chem. Soc., Faraday Trans.* **1994**, *90*, 1073−1076.
(17) Drain, C. M.; Kirmaier, C.; Medforth, C. J.; Nurco, D. J.; Smith, K. M.; Holten, D. *J. Phys. Chem.* **1996**, *100*, 11984−11993.
(18) Takeda, J.; Ohya, T.; Sato, M. *Chem. Phys. Lett.* **1991**, *183*, 384−386.
(19) Medforth, C. J.; Senge, M. O.; Smith, K. M.; Sparks, L. D.; Shelnutt, J. A. *J. Am. Chem. Soc.* **1992**, *114*, 9859−9869.
(20) Barkigia, K. M.; Berber, M. D.; Fajer, J.; Medforth, C. J.; Renner, M. W.; Smith, K. M. *J. Am. Chem. Soc.* **1990**, *112*, 8851−8857.
(21) Ema, T.; Senge, M. O.; Nelson, N. Y.; Ogoshi, H.; Smith, K. M. *Angew. Chem., Int. Ed. Engl.* **1994**, *33*, 1879−1881.
(22) Jentzen, W.; Simpson, M. C.; Hobbs, J. D.; Song, X.; Ema, T.; Nelson, N. Y.; Medforth, C. J.; Smith, K. M.; Veyrat, M.; Mazzanti, M.; Ramasseul, R.; Marchon, J.-C.; Takeuchi, T.; Goddard, W. A., III; Shelnutt, J. A. *J. Am. Chem. Soc.* **1995**, *117*, 11085−11097.

18-octaethylporphyrin (OEP).[12−14,23] Representative compounds in this class are shown below. The metalated complexes Zn-(T(*t*-Bu)P), Zn(DPP), and Zn(OETPP) also exhibit photophysical properties which differ markedly with respect to Zn(TPP).[14] Thus, potential excited-state relaxation mechanisms involving tautomerism or proton transfer in the free bases were discounted. Moreover, at low temperature and in frozen matrices, the emission behavior for each of the sterically encumbered nonplanar porphyrins approaches that observed for planar porphyrins.[12,13] These considerations led to the proposal that conformational dynamics in the $^1(\pi,\pi^*)$ state involving thermal population of low-frequency out-of-plane vibrational modes of the macrocycle underlie excited-state relaxation.[14]
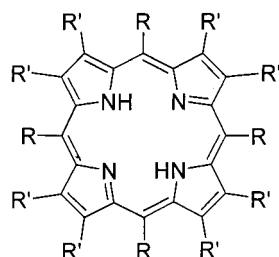
| Porphyrin	R	R'
T(t-Bu)P	$(CH_3)_3C$	H
DPP	C_6H_5	C_6H_5
OETPP	C_6H_5	CH_3CH_2

In stark contrast to the above studies, electron-deficient 5,-10,15,20-tetrakis(perfluoroalkyl)porphyrins (TR_fP)[24] are non-planar, but exhibit hypsochromic absorption spectra, sharp emission bands, and small Stokes shifts typical of normal planar porphyrins, such as TPP.[15] The fluorescence quantum yields of TR_fPs are reduced by a factor of 3 compared to TPP, and the S_1 lifetimes are only reduced by a factor of 7. The differences between the metalated complexes $Zn(TC_3F_7P)$ ($\phi_f = 0.013$, $\tau_f = 1.2$ ns, THF) and Zn(TPP) ($\phi_f = 0.033$, $\tau_f = 1.86$ ns, THF) are smaller still.[15]

Thus, the photophysics of two classes of sterically encumbered, nonplanar porphyrins, the electron-rich T(*t*-Bu)P, DPP, and OETPP and the electron-poor TR_fPs, are dramatically different: the former class exhibits highly "perturbed" opto-electronic behavior, while the latter does not. The current understanding of the stereoelectronic consequences of porphyrin ring distortion is unable to explain the disparity in these spectroscopic studies. It is important to be able to reconcile these data if one is to understand the photophysics of protein-bound porphyrin-derived pigments and how macrocycle structure modulates the electronic properties in the panoply of heme protein active sites in biology.

β-Octafluoro-*meso*-tetraarylporphyrins (F$_8$TPP and F$_{28}$TPP) are structurally intriguing compounds. It is clear from semiempirical calculations (AM1),[25] which predict relatively minor endotherms for small excursions from planarity, that the planar conformation resides on a shallow potential energy surface.[26] The ease with which β-octafluoro-*meso*-tetraarylporphyrins can be deformed has its origins in the substantial steric interactions between the β-fluorine substituents and the aryl residues at the

porphyrin periphery (C−F contacts ∼2.8 Å). Consequently, these compounds are useful and sensitive probes of excited-state conformational dynamics.

Here, we present the structural characterization of Zn(F$_8$TPP) and photophysical studies of two sterically encumbered β-octafluoroporphyrins and their zinc complexes.[26,27] A key point from these studies is that remarkably disparate excited-state behavior is observed for the octafluorinated (F$_8$TPP) and perfluorinated (F$_{28}$TPP) porphyrins, possessing similar absorption spectra. This observation indicates that current theory, relating porphyrin ring conformation to their optoelectronic properties, may need to be expanded upon or revisited.
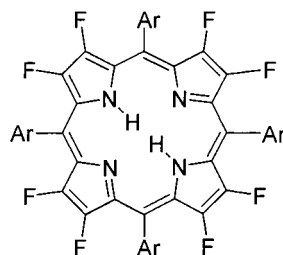
F$_8$TPP. Ar = C$_6$H$_5$
F$_{28}$TPP. Ar = C$_6$F$_5$
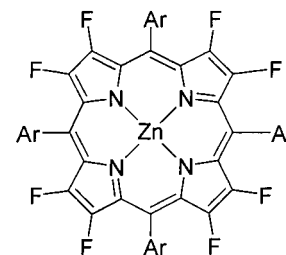
Zn(F$_8$TPP). Ar = C$_6$H$_5$
Zn(F$_{28}$TPP). Ar = C$_6$F$_5$

Experimental Section

Materials. Methylene chloride and benzonitrile were distilled from calcium hydride, the latter under reduced pressure. F$_8$TPP and F$_{28}$TPP, and their zinc complexes were prepared as described previously.[26]

Photophysical Studies. Absorption spectra were obtained using an OLIS-14 modification of a Carey-14 UV-vis−NIR spectrometer. Steady-state fluorescence spectra were measured on a SPEX fluorolog using optically dilute samples. Optical densities at excitation wavelengths were 0.03. Fluorescence decay measurements were performed on ∼1 × 10^{-5} M solutions by the time-correlated single photon counting method. The excitation source was a cavity-dumped Coherent 700 dye laser pumped by a frequency doubled Coherent Antares 76s Nd:YAG laser.[28] The instrument response function was 35 ps, as measured at the excitation wavelength for each decay experiment with Ludox AS-40. Nanosecond transient absorption measurements were made with excitation from an Opotek optical parametric oscillator pumped by the third harmonic of a Continuum Surelite Nd:YAG laser. The pulse width was ∼5 ns, and the repetition rate was 5 Hz. The detection portion of this system has been described elsewhere.[29] Detection of singlet oxygen phosphorescence was via a North Coast Scientific Ge detector (EO-817PP). All samples were saturated with oxygen, and disparities in ground-state absorption at excitation wavelengths were corrected.

Steady-state fluorescence and singlet oxygen quantum yields were calculated using the comparative method.[30] The calculation was as follows:

$$X^u/X^r = (\Phi^u OD^u)/(\Phi^r OD^r)$$

where X is the integrated fluorescence areas for the fluorescence quantum yields and the excited-state luminescence counts in the singlet oxygen calculations. The unknown is denoted by "u" and the reference

(23) Retsek, J. L.; Gentemann, S.; Medforth, C. J.; Smith, K. M.; Chirvony, V. S.; Fajer, J.; Holten, D. *J. Phys. Chem. B* **2000**, *104*, 6690−6693.

(24) DiMagno, S. G.; Williams, R. A.; Therien, M. J. *J. Org. Chem.* **1994**, *59*, 6943−6948.

(25) Dewar, M. J. S.; Zoebisch, E. G.; Healy, E. F.; Stewart, J. J. P. *J. Am. Chem. Soc.* **1985**, *107*, 3902−3909.

(26) Woller, E. K.; DiMagno, S. G. *J. Org. Chem.* **1997**, *62*, 1588−1593.

(27) Leroy, J.; Bondon, A.; Toupet, L.; Rolando, C. *Chem. Eur. J.* **1997**, *3*, 1890−1893.

(28) Gust, D.; Moore, T. A.; Luttrull, D. K.; Seely, G. R.; Bittersman, E.; Bensasson, R. V.; Rougee, M.; Land, E. J.; de Schryver, F. C.; Van der Auweraer, M. *Photochem. Photobiol.* **1990**, *51*, 419−426.

(29) Davis, F. S.; Nemeth, G. A.; Anjo, D. M.; Makings, L. R.; Gust, D.; Moore, T. A. *Rev. Sci. Instrum.* **1987**, *58*, 1629−1631.

(30) Bensasson, R. V.; Land, E. J.; Truscott, T. G. *Photolysis and Pulse Radiolysis: Contributions to the Chemistry of Biology and Medicine*; Pergamon: Oxford, 1983.
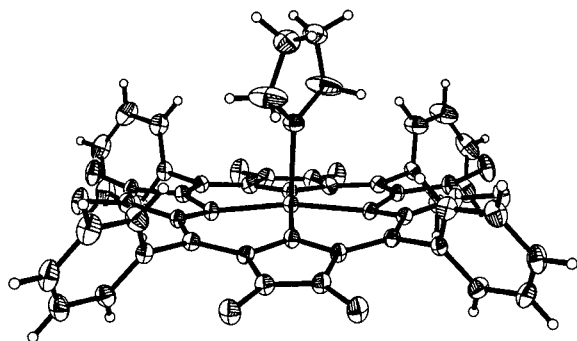
Figure 1. Perspective drawing from the X-ray crystal structure determination of Zn(F$_8$TPP)·THF with thermal ellipsoids at 25 % probability.

compound is "r". *OD* is the ground-state absorption at the excitation wavelengths for both experiments, and Φ is the singlet oxygen fluorescence quantum yield. Luminescence signals were linear with respect to the excitation energy for all singlet oxygen calculations.

X-ray Diffraction Studies of Zn(F$_8$TPP)·THF. Crystals of Zn(F$_8$-TPP)·THF were obtained by slow evaporation (3 weeks) of a THF:octane 1:1 solution (30 mg of Zn(F$_8$TPP) in 80 mL) at room temperature. A deep red, flat block crystal, of approximate dimensions 0.4 × 0.4 × 0.2 mm, was sealed in a glass capillary (to prevent loss of solvent) for collection of diffraction data. All measurements were performed with graphite monochromated Ag Kα radiation ($\lambda = 0.5608$ Å) produced by a Siemens rotating-anode X-ray source. Data were collected at room temperature by the oscillation method using a MARResearch (18 cm) imaging plate area detector. The data were processed using the MARXDS program.[31] Data were corrected for Lorentz and polarization factors, but not for absorption. A total of 19662 reflections were measured and averaged to 5298 unique reflections (R_{int} = 0.0438). Structure solution and refinement were carried out using the SHELX-97 package of programs.[32] The structure was solved in the monoclinic space group $P2_1/n$ by Patterson methods. After determination of the location of the zinc ion, subsequent iterations of difference Fourier synthesis followed by determination of the heavy atom positions led to the location of all heavy atoms. All non-hydrogen atoms were refined anisotropically. Hydrogen atom positions were determined by idealized geometries and treated as riding atoms. At convergence, $R_1 = 0.0693$ (for 4700 reflections with $F_o > 4\sigma(F_o)$), $wR_2 = 0.1755$, and GOF = 1.185. A final difference Fourier map was judged to be significantly free of features, with the largest positive peak having a height of 1.11 e/Å^3 and the lowest negative peak having a height of 0.30 e/Å^3.

Results

X-ray Crystal Structure of Zn(F$_8$TPP)·THF. Crystals of Zn(F$_8$TPP)·THF suitable for X-ray diffraction were grown by the slow evaporation of a THF/octane solution; the compound obtained from this process was a five-coordinate THF adduct. A perspective drawing from the crystal structure determination is shown in Figure 1, and average bond lengths and angles are given in Table 1. The zinc atom is displaced by 0.17 Å from the plane of the porphyrin ring in the direction of the coordinated THF molecule. The Zn–O bond is short, (2.147 Å), accurately reporting the electron deficient nature of the porphyrin. The Zn–N bond lengths (2.063 Å average) are in the range expected for nearly planar zinc complexes, but are long in comparison to those reported for the saddled compounds Zn(Cl$_8$TFPP), (2.032 Å), and Zn(Br$_8$TFPP), (2.040 Å).[35,36] The most note-

worthy aspect of the structure of Zn(F$_8$TPP)·THF is the large degree of nonplanarity of the porphyrin ring. The porphyrin ring is extensively saddled; the largest deviations of carbon atoms from the porphyrin mean plane (0.43 Å average) occur at the β-pyrrole positions. Superimposed upon this distortion mode is a second, smaller ruffling of the porphyrin core. These gross features of the ring distortion in Zn(F$_8$TPP)·THF are very similar to those observed for other β-octahalotetraarylporphyrins; however, the structures of Zn(Cl$_8$TFPP) and Zn(Br$_8$TFPP) show larger displacements of the β-pyrrole carbon atoms from the porphyrin mean planes.[35,36] The smaller degree of nonplanar distortion observed in Zn(F$_8$TPP)·THF stems from the mitigated aryl–halogen steric interactions at the porphyrin periphery; fluorine has a substantially reduced van der Waals radius compared to the heavier halogens.[37]

A comparison of the structure of Zn(F$_8$TPP)·THF to that recently reported for Zn(F$_8$TPP)·H$_2$O[27] reveals that the axial ligand plays an extremely modest role in modulating the solid-state conformation of the porphyrin core. The aquo complex of Zn(F$_8$TPP) exhibits a more pronounced saddle distortion (0.59 Å average displacement of the pyrrole β-positions) and a shorter Zn–O contact (2.092 Å) than Zn(F$_8$TPP)·THF. The remaining structural parameters (Table 1) are identical, within experimental error. The small changes induced in the structure of Zn(F$_8$TPP) by altering (or removing) the axial ligand are also consistent with recent theoretical predictions.[38]

Although the structure of Zn(F$_8$TPP)·THF follows the trends observed for Zn(Cl$_8$TFPP) and Zn(Br$_8$TFPP), it is quite dissimilar to the previously reported structure of five-coordinate Zn(F$_{28}$TPP), in which the porphyrin ring is essentially flat.[26] (Planar structures are also obtained for the free base and the Co(II) and Rh(III) complexes of F$_{28}$TPP.)[39–41] It is curious that Zn(F$_{28}$TPP) and Zn(F$_8$TPP) should show such different solid-state structures. It is clear that these fluorinated porphyrins reside on shallow conformational potential energy surfaces, that crystal packing forces are different for Zn(F$_8$TPP)·THF and Zn(F$_{28}$-TPP), and that the ability of crystal packing forces to distort even sterically unencumbered porphyrins is well documented.[42] Thus, crystal packing forces cannot be discounted as the origin for the structural dissimilarities of Zn(F$_8$TPP)·THF and Zn(F$_{28}$-TPP).

A second potential explanation for the structural differences between Zn(F$_8$TPP)·THF and Zn(F$_{28}$TPP) can be found in the details of β-fluorine-aryl interactions in the two fluorinated zinc complexes. In the structure of Zn(F$_8$TPP)·THF, the nonbonded C–F contacts (e.g., F3–C21) average 2.82 Å, as compared to 2.77 Å for the corresponding nonbonded contacts in Zn(F$_{28}$-TPP). For F$_8$TPP and Zn(F$_8$TPP), the electrostatic contribution to the interaction of the β-fluorines with the (negatively charged) face of a *meso*-phenyl substituent should be quite unfavorable. In contrast, the same β-fluorine-aryl interaction with a *meso*-

(31) Kabsch, W. *J. Appl. Crystallogr.* **1988**, *21*, 916.

(32) Sheldrick, G. M. *SHELX-97*; University of Gottingen, 1997.

(33) Schauer, C. K.; Anderson, O. P.; Eaton, S. S.; Eaton, G. R. *Inorg. Chem.* **1985**, *24*, 4082–4086.

(34) Scheidt, W. R.; Kastner, M. E.; Hatano, K. *Inorg. Chem.* **1978**, *17*, 706–710.

(35) Birnbaum, E. R.; Hodge, J. A.; Grinstaff, M. W.; Schaefer, W. P.; Henling, L.; Labinger, J. A.; Gray, H. B. *Inorg. Chem.* **1995**, *34*, 3625–3632.

(36) Marsh, R. E.; Schaefer, W. P.; Hodge, J. A.; Hughes, M. E.; Gray, H. B.; Lyons, J. E.; Ellis, P. E. *J. Acta Crystallogr.* **1993**, *C49*, 1339–1342.

(37) Bondi, A. *J. Phys. Chem.* **1964**, *68*, 441–451.

(38) Nguyen, K. A.; Day, P. N.; Pachter, R. *J. Phys. Chem. A* **1999**, *103*, 9378–9382.

(39) Leroy, J.; Bondon, A.; Toupet, L. *Acta Crystallogr.* **1999**, *C55*, 464–466.

(40) Smirnov, V. V.; Woller, E. K.; DiMagno, S. G. *Inorg. Chem.* **1998**, *37*, 4971–4978.

(41) Nelson, A. P.; DiMagno, S. G. *J. Am. Chem. Soc.* **2000**, *122*, 8569–8570.

(42) Scheidt, W. R.; Lee, Y. J. *Struct. Bond.* **1987**, *64*, 1–70.

Table 1. Average Bond Lengths (Å) and Bond Angles (Deg) for Zn(F$_8$TPP)·THF and Selected Zinc Porphyrins

parameter	Zn(F$_8$TPP)·THF	Zn(F$_{28}$TPP)·THF	Zn(F$_8$TPP)·H$_2$O	Zn(TPP)·2THF	Zn(TPP)	Zn(TFPP)	Zn(Cl$_8$TFPP)	Zn(Br$_8$TFPP)
N−Zn	2.063(4)	2.059(6)	2.068(5)	2.057(2)	2.036(2)	2.036(2)	2.032(11)	2.038(21)
N−C$_\alpha$^{a}	1.381(7)	1.382(10)	1.372(8)	1.371(4)	1.375(2)	1.371(3)	1.380(13)	1.375(23)
C$_\alpha$−C$_\beta$^{b}	1.440(8)	1.439(12)	1.429(9)	1.444(5)	1.443(3)	1.438(4)	1.427(16)	1.450(26)
C$_\beta$−C$_\beta$	1.328(8)	1.337(12)	1.320(10)	1.349(4)	1.351(3)	1.339(4)	1.337(15)	1.352(28)
C$_\alpha$−C$_m$^{c}	1.395(8)	1.397(12)	1.393(9)	1.403(4)	1.399(3)	1.398(3)	1.403(15)	1.392(26)
C$_\alpha$−N−C$_\alpha$	108.2(4)	107.4(6)	108.5(5)	107.0(3)	106.5(1)	106.2(2)	106.9(8)	109.1(16)
N−C$_\alpha$−C$_\beta$	107.5(5)	108.3(7)	107.3(5)	109.3(3)	109.6(2)	109.6(2)	107.4(9)	107.6(14)
N−C$_\alpha$−C$_m$	126.1(5)	125.5(7)	126.1(6)	125.8(3)	125.7(2)	125.1(2)	124.2(9)	124.6(16)
C$_\alpha$−C$_\beta$−C$_\beta$	108.4(5)	108.0(8)	108.4(6)	107.2(3)	107.2(2)	107.3(2)	108.8(10)	107.7(17)
C$_\alpha$−C$_m$−C$_\alpha$	124.5(5)	126.0(8)	124.5(6)	125.0(3)	125.0(2)	126.1(2)	126.5(10)	124.0(17)
reference	this work	26	27	33	34	35	35	36

^{a} Carbon atoms in α-positions of pyrrole rings. ^{b} Carbon atoms in β-positions of pyrrole rings. ^{c} Carbon atoms in *meso*-positions of porphyrin ring.

Table 2. Optical Spectroscopy, Fluorescence, and Photophysics of *β*-Octafluorinated Porphyrins in Benzonitrile, with Data for Selected Porphyrins

compd	λ_{max} (absorbance) (nm)	Q(0,0)/ Q(1,0)^a	λ_{max} (fluor) (nm)	Stokes Shift (cm^{-1})	Φ_f^{b}	S$_1$ lifetime (ns)^c	k_{obs} (10^{8}s^{-1})	k_f (10^7 s^{-1})	k_{ic} (10^{8}s^{-1})	k_{isc} (10^8 s^{-1})	Φ_T (O$_2$)^d	τ_T (μs)^e
F$_8$TPP	409, 502, 535, 584, 639	1.29	662 (br)	544	0.06	2.97	3.37	2.02	0.408	2.76	0.82	26
F$_{28}$TPP	399, 498, 534, 579, 632	0.07	640, 702	198	0.03	6.26	1.60	0.48	0.400	1.15	0.72	775
TPP	422, 516, 552, 592, 649	0.80	652, 716	71	0.11^f	10.6^g	0.94	1.04	0.21	0.63	0.67	120
Zn(F$_8$TPP)	417, 547, 585	0.45	610, 639	701	0.018	0.445	22.5	4.04	5.20	16.9	0.75	63
Zn(F$_{28}$TPP)	416, 544, 585	0.003	592, 637	202	0.019	1.09	9.17	1.74	2.21	6.76	0.74	2150
Zn(TPP)	429, 560, 600	0.42	607, 658	192	0.032^h	2.2^h	4.54	1.43	0.397	4.0	0.88	
DPP^i	718		772 (br)	975	0.006	0.83	12.05	0.72	<5.88	>5.88	>0.5	
T(t-Bu)P^j	696		720	478	2 × 10^{-4}	0.046	217	0.63	>333	>83.3	<0.2	
Zn(DPP)^k				1360	0.010	0.5	20	2	<9.8	>10	>0.5	
Zn(T(t-Bu)P)^k				1300	3 × 10^{-5}	0.007	1428	0.43			−^{l}	
TC$_3$F$_7$P^m	405, 510, 544, 593, 647	2.19	651, 717	126	0.028	1.4	7.14	2				
Zn(TC$_3$F$_7$P)^n	409, 554, 593	1.91	607, 652	384	0.013	1.2	8.33	1.08				

^{a} Defined as the extinction coefficient of the lowest energy absorption band divided by the extinction coefficient for the lowest energy first vibrational overtone, as discussed in ref 47. ^{b} Fluorescence quantum yields measured in the steady state using hematoporphyrin dimethyl ester (HPDME) as a standard (Φ_f=0.09). HPDME was in methanol. Samples were not purged with Ar. ^{c} Samples were not purged with Ar. ^{d} Triplet yields determined assuming 100% singlet oxygen sensitization. Quantum yields of singlet oxygen sensitization were measured by emission at 1270 nm. Linear dependence with respect to laser energy was verified, and samples were in oxygen saturated benzonitrile. Reference for F$_8$TPP and F$_{28}$TPP was TPP, and for Zn(F$_8$TPP) and Zn(F$_{28}$TPP) was HPDME. ^{e} Triplet lifetimes measured in argon purged benzonitrile. ^{f} In benzene, ref 48. ^{g} In methanol, ref 49. ^{h} In toluene, ref 50. ^{i} In toluene, ref 12. ^{j} In 3-methylpentane/isopentane = 1/1, ref 13. ^{k} In 2-methyltetrahydrofuran, ref 14. ^{l} Very low, ref 14. ^{m} In CH$_2$Cl$_2$, ref 15. ^{n} In THF, ref 15.

pentafluorophenyl group should have a less unfavorable (and perhaps attractive) electrostatic contribution in F$_{28}$TPP and Zn-(F$_{28}$TPP). Thus, the reversed quadrupolar charge distributions of the phenyl and perfluorophenyl substituents (as in hexafluorobenzene and benzene[43-46]) may be responsible for the differing solid-state structures of Zn(F$_8$TPP)·THF and Zn(F$_{28}$TPP). This argument is congruent with the observation that the structures of F$_{28}$TPP and its metal chelates reported to date show more planar macrocycle conformations than the corresponding F$_8$-TPP derivatives.

Optical Spectroscopy. The absorption data for the fluorinated porphyrin derivatives are given in Table 2. The Soret (B) bands are *hypsochromically* shifted compared to all other tetraarylporphyrins, but are still lower in energy than the B-band of porphine. The lowest energy (Q) bands are also hypsochromically shifted compared to TPP, and these blue shifts are similar to that of planar octaalkyltetraarylporphyrins.[51] The shifts of the absorption bands to higher energy may arise from the

π-electron donation from the *β*-fluorines, which disproportionately destabilizes the e$_g$ LUMO orbitals in Gouterman's four orbital model.[52] A similar effect is responsible for the extremely high energy Soret band noted for 2,3,7,8,12,13,17,18-octamethoxyporphyrin.[53] Additionally, the increased orthogonality of the aryl rings, particularly seen in the structure of Zn(F$_{28}$-TPP), may contribute to the blue shifting in the optical spectra by minimizing conjugative interactions at the *meso*-positions.[54]

The relative intensities of the Q(0,0) and Q(1,0) absorption transitions are strikingly different for the octafluorinated and perfluorinated porphyrins (Figure 2). Gouterman has related the

(43) Coates, G. W.; Dunn, A. R.; Henling, L. M.; Dougherty, D. A.; Grubbs, R. H. *Angew. Chem., Int. Ed. Engl.* **1997**, *36*, 248−251.
(44) Williams, J. H. *Acc. Chem. Res.* **1993**, *26*, 593−598.
(45) Patrick, C. R.; Prosser, G. S. *Nature* **1960**, *187*, 1021.
(46) Dahl, T. *Acta Chem. Scand.* **1994**, *48*, 95−106.

(47) Spellane, P. J.; Gouterman, M.; Antipas, A.; Kim, S.; Liu, Y. C. *Inorg. Chem.* **1980**, *19*, 386-391.
(48) Seybold, P. S.; Gouterman, M. *J. Mol. Spectrosc.* **1969**, *31*, 1−13.
(49) Bonnett, R.; McGarvey, D. J.; Harriman, A.; Land, E. J.; Truscott, T. G.; Winfield, U. J. *Photochem. Photobiol.* **1988**, *48*, 271−276.
(50) Grayushko, A. T.; Tsvirko, M. P. *Opt. Spectrosc.* **1971**, *31*, 291−295.
(51) Senge, M. O.; Medforth, C. J.; Sparks, L. D.; Shelnutt, J. A.; Smith, K. M. *Inorg. Chem.* **1993**, *32*, 1716−1723.
(52) Gouterman, M. *J. Mol. Spectrosc.* **1961**, *6*, 138−163.
(53) Merz, A.; Schropp, R.; Lex, J. *Angew. Chem., Int. Ed. Engl.* **1993**, *32*, 291−293.
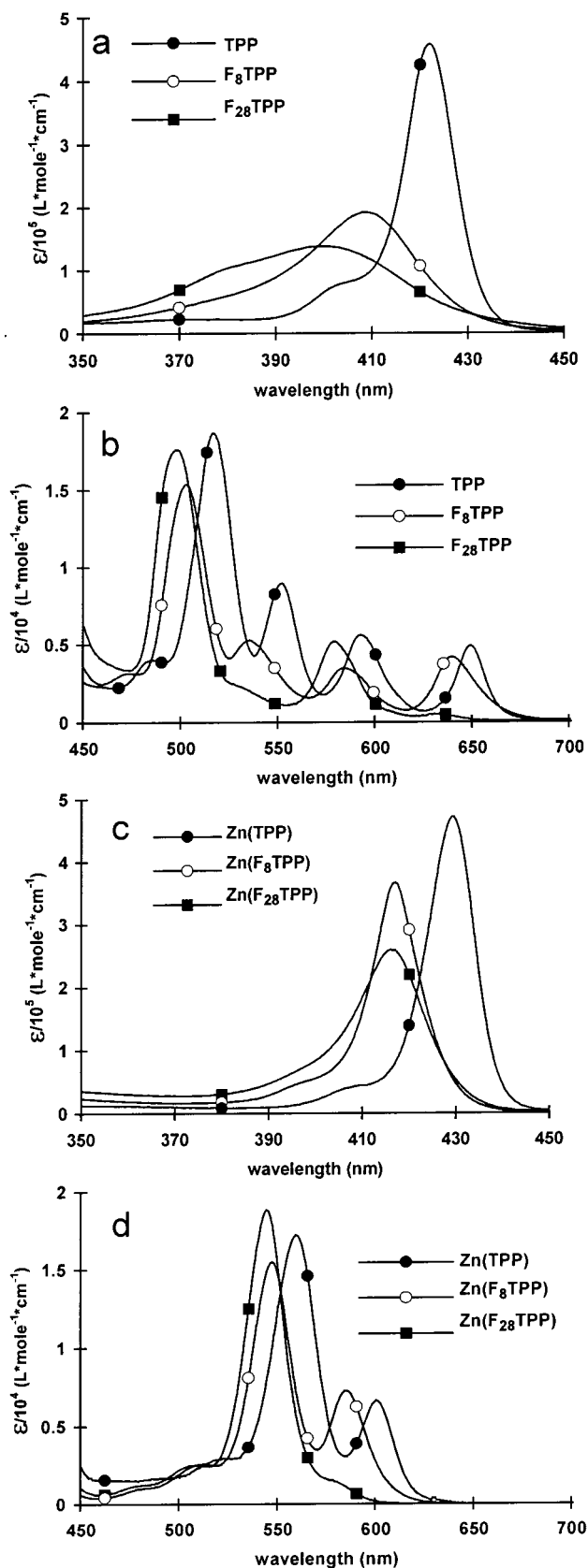(54) DiMagno, S. G.; Wertsching, A. K.; Ross, C. R., II *J. Am. Chem. Soc.* **1995**, *117*, 8279−8280.

Figure 2. Normalized optical absorption spectra of TPP, Zn(TPP), F$_8$TPP, Zn(F$_8$TPP), F$_{28}$TPP, and Zn(F$_{28}$TPP) in benzonitrile: (a) B-band region for free base porphyrins, (b) Q-band region for free base porphyrins, (c) B-band region for zinc porphyrins, (d) Q-band region for zinc porphyrins.

intensities of these absorption bands {$A[Q(0,0)]/A[Q(1,0)]$} to the degree of degeneracy in the highest lying ($a_{1u} \rightarrow e_g$ and

$a_{2u} \rightarrow e_g$) transitions according to eq 1, where $^1E(a_{2u} \rightarrow e_g)$ and $^1E(a_{1u} \rightarrow e_g)$ are the energies of the two single transitions.[47] Thus,

$$A[Q(0,0)]/A[Q(1,0)] = (\text{const})[^1E(a_{2u} \rightarrow e_g) - {}^1E(a_{1u} \rightarrow e_g)]^2$$

(1)

the small Q(0,0) extinction coefficients for F$_{28}$TPP and Zn(F$_{28}$-TPP) indicate energetically degenerate a_{1u} and a_{2u} filled frontier orbitals. In contrast, the Q(0,0) bands for F$_8$TPP and Zn(F$_8$-TPP) have significant oscillator strengths and Q(0,0)/Q(1,0) intensity ratios similar to that of the TPP derivatives. Elementary substituent effect arguments (phenyl is a significantly better electron-donating group than pentafluorophenyl)[55] predict HO-MOs for F$_8$TPP and Zn(F$_8$TPP) that are predominantly a_{2u} in character.

Although there are small differences in the energies of the absorption bands for the free bases F$_8$TPP and F$_{28}$TPP, the positions of the absorption maxima for the zinc derivatives are virtually superimposable. Using conventional theories of porphyrin stereoelectronic effects, in which nonplanar distortions are correlated with dramatic red shifts in the optical spectra, these data would suggest that the two fluorinated porphyrins are nearly isostructural (and planar) in benzonitrile. According to this analysis, one would expect no dramatic differences in the excited-state properties of the octafluorinated and perfluorinated derivatives. To test whether there were discernible differences between the solid-state and solution structures of Zn(F$_8$TPP), we compared the optical spectra of crystalline F$_8$-TPP, Zn(F$_8$TPP), F$_{28}$TPP, Zn(F$_{28}$TPP), TPP, and Zn(TPP) in the solid state (in a KBr pellet)[54] to the spectra of the same compounds in CH$_2$Cl$_2$ and benzonitrile (see Supporting Information). Transfer of F$_8$TPP and Zn(F$_8$TPP) to solution resulted in shifts of the optical absorption bands that were not discernibly different from those observed for transfer of F$_{28}$TPP and Zn-(F$_{28}$TPP) from the solid state to solution. Were optical spectra correlated with porphyrin nonplanarity, the results of the solid-state and solution spectroscopic studies would lead to the conclusion that the nonplanar solid-state structure of Zn(F$_8$TPP) is maintained in solution. However, the same posited correlation between porphyrin nonplanarity and optical absorption spectroscopy leads to the opposite conclusion that Zn(F$_8$TPP) and Zn(F$_{28}$TPP) should have similar structures. Clearly, these two conclusions cannot be simultaneously true, since there are clear structural differences between Zn(F$_8$TPP) and Zn(F$_{28}$TPP) in the solid state. Thus, the anticipated red shifts in optical spectra associated with ring distortion in porphyrins must be absent in these electron-deficient derivatives, and no structural information may be inferred from a comparison of optical absorption spectra alone. In this situation, excited-state properties could provide valuable information regarding the solution conformations of these fluorinated porphyrins.

Fluorescence Spectroscopy. Despite the similarities in the ground-state absorption spectra of the octafluorinated and perfluorinated porphyrins, the steady-state emission data are remarkably different (Table 2). TPP, Zn(TPP), F$_{28}$TPP, and Zn-(F$_{28}$TPP) exhibit emission spectra with small Stokes shifts and fine structures that mirror the absorption spectra in intensity and spacing. These aspects of the porphyrin emissions indicate that the compounds do not undergo significant reorganization of nuclear coordinates in the excited state. Compounds F$_8$TPP and Zn(F$_8$TPP) show broad, relatively featureless emission spectra and substantial Stokes shifts. These data are reminiscent

(55) Hansch, C.; Leo, A.; Taft, R. W. *Chem. Rev.* **1991**, *91*, 165−195.

of the emission spectra of distorted porphyrins with a_{2u} ground states, such as T(*t*-Bu)P and OETPP,[12−14] and indicate that there is substantial excited-state conformational reorganization. The excited-state conformational reorganization for F_8TPP and Zn-(F_8TPP) appears to be intrinsic to the ring system and independent of the solvent, since comparable Stokes shifts are also observed in the emission spectra of methylene chloride solutions (see Supporting Information).

The quantum yields of fluorescence of the *β*-octafluorinated compounds are slightly diminished from those of TPP and Zn-(TPP), but F_8TPP, Zn(F_8TPP), F_{28}TPP, and Zn(F_{28}TPP) still possess impressive yields for extremely electron-deficient porphyrins, resembling *meso*-tetrakis(perfluoroalkyl)porphyrins in this regard. In contrast, chlorinated and brominated tetraarylporphyrin derivatives exhibit sharply reduced fluorescence quantum yields.[56,57] Within the set of *β*-octafluorinated porphyrins, it is interesting to note that the fluorescence quantum yield of F_8TPP exceeds that of F_{28}TPP. This result is consistent with the reduced integrated oscillator strength of F_{28}TPP in the Q-band region compared to that of F_8TPP (Figure 2). The similar quantum yields of fluorescence for Zn(F_8TPP) and Zn(F_{28}TPP) result from a combination of factors, which are discussed below.

The fluorescence lifetimes of the fluorinated compounds are reduced from those of TPP, with F_8TPP and Zn(F_8TPP) exhibiting the most precipitous drop. Nevertheless, the radiative lifetimes are quite long in comparison to other extremely electron-deficient porphyrins.[15,58] The radiative rates of F_8TPP, Zn(F_8TPP), F_{28}TPP, and Zn(F_{28}TPP) were calculated from the S_1 lifetimes and the quantum yield of fluorescence ($k_f = \phi_f/\tau_f$, Table 2). The larger radiative rate constants measured for F_8-TPP and Zn(F_8TPP) relative to F_{28}TPP and Zn(F_{28}TPP) are consistent with the larger integrated oscillator strength for the Q-bands of the octafluorinated derivatives.

The magnitudes of the remaining excited-state deactivation rate constants (k_{isc} and k_{ic}) were determined from the quantum yields for triplet formation and nonradiative events, respectively. Increased rates of intersystem crossing and internal conversion are characteristics generally observed for nonplanar porphyrins possessing a_{2u} HOMOs,[12] and this relationship also seems to hold for *β*-octafluorinated porphyrins. The increased nonplanarity of F_8TPP and Zn(F_8TPP) is manifested in slightly faster rates of intersystem crossing and internal conversion, in comparison to F_{28}TPP and Zn(F_{28}TPP).

Discussion

The data presented here indicate that F_8TPP and Zn(F_8TPP) bear the photophysical signatures of nonplanar porphyrins, while F_{28}TPP and Zn(F_{28}TPP) do not. The available structural data and the disparate excited-state behavior are consistent with nonplanar ground-state solution conformations for F_8TPP and Zn(F_8TPP) and planar solution conformations for F_{28}TPP and Zn(F_{28}TPP). As discussed above, such behavior is not altogether consistent with the current quasitheoretical treatments relating optical absorption spectra to the ground-state conformations of porphyrins, and suggests that excited-state properties might be more sensitive and reliable diagnostic indicators of the porphyrin ground-state conformation than absorption spectra.

The correlation of porphyrin ring conformations with excited-state properties is obviously not 100% reliable, as the data in

Table 2 show. Particularly noteworthy is the lack of a significant Stokes shift observed for TC_3F_7P or Zn(TC_3F_7P); why these compounds differ significantly from the other nonplanar porphyrins listed in Table 2 remains an open question. The compounds listed in Table 2 exhibit different nonplanar distortion modes (DPP and Zn(DPP) are saddled, T(*t*-BuP), ZnT(*t*-BuP), TC_3F_7P, and Zn(TC_3F_7P) are ruffled), so the distortion mode can be eliminated as a possible explanation for the unusual photophysical properties of TC_3F_7P and Zn(TC_3F_7P). Similarly, the redox potentials of the compounds in Table 2 span a wide range, but the fact that the nonplanar electron-deficient porphyrins F_8TPP and Zn(F_8TPP) exhibit excited-state behavior that mirrors other nonplanar porphyrins, while TC_3F_7P and Zn-(TC_3F_7P) do not, seems to rule out porphyrin ring electron density as a cause for the unusual properties of the latter compounds. One feature that distinguishes TC_3F_7P and Zn-(TC_3F_7P) from the remaining compounds in Table 2 is that their ground-state electronic structure is different; they are predicted to possess a_{1u} HOMOs rather than a_{2u} HOMOs. Were ground-state electronic structure correlated with the type and degree of excited-state conformational change, the dilemma concerning the divergent photophysical behavior of nonplanar porphyrins would be resolved. Such a hypothesis could provide a general explanation for the interesting differences observed in the excited-state behavior of nonplanar TR_fPs and other highly substituted model compounds. Moreover, such proposals are attractive targets for theoretical inquiry.

Conclusion

The sterically encumbered porphyrins F_8TPP and F_{28}TPP occupy an interesting position between nonplanar porphyrins, featuring electron-donating *meso*-substituents and a_{2u} HOMOs, and nonplanar *meso*-tetrakis(perfluoroalkyl)porphyrins, for which empirical and theoretical studies indicate a_{1u} HOMOs.[15,54] The steric interactions at the periphery of the octafluorinated porphyrins are balanced by the countervailing electronic preference for planarity. Thus, these compounds are exquisite models to probe the sensitivity of porphyrin excited states to steric and electronic effects. As the studies reported herein show, minimal changes in the substituent steric parameters lead to surprisingly large differences in the excited-state properties of these pigments, given their similar optical spectra. These studies highlight that it is impossible to predict the optoelectronic behavior of porphyrins within the current theoretical framework.

Supporting Information Available: Listing of X-ray structural information including crystal data, atomic coordinates, and bond lengths and angles for Zn(F_8TPP)·THF, emission spectra for the F_8TPP, Zn-(F_8TPP), F_{28}TPP, Zn(F_{28}TPP), TPP, and Zn(TPP) in CH_2Cl_2 and benzonitrile, and absorption data for F_8TPP, Zn(F_8TPP), F_{28}TPP, and Zn(F_{28}TPP) in CH_2Cl_2, benzonitrile, and in the solid state. This material is available free of charge via the Internet at http://pubs.acs.org.

IC001116Z

(56) Bonnett, R.; Harriman, A.; Kozyrev, A. N. *J. Chem. Soc., Faraday Trans.* **1992**, *88*, 763−769.

(57) Quimby, D. J.; Longo, F. R. *J. Am. Chem. Soc.* **1975**, *97*, 5111−5117.

(58) Bhyrappa, P.; Krishnan, V. *Inorg. Chem.* **1991**, *30*, 239−245.